Turkish Journal of Electrical Engineering & Computer Sciences

http://journals.tubitak.gov.tr/elektrik/

Research Article

Turk J Elec Eng & Comp Sci
(2019) 27: 258 – 273

doi:10.3906/elk-1803-134

Evaluation of power system robustness in order to prevent cascading outages

Farnaaz HAJBANI[*], **Heresh SEYEDI**, **Kazem ZARE**
Faculty of Electrical and Computer Engineering, University of Tabriz, Tabriz, Iran

Received: 19.03.2018 • **Accepted/Published Online:** 06.07.2018 • **Final Version:** 22.01.2019

Abstract: Power system robustness against overload condition is a challenging issue in the fields of power system planning and operation. In this paper, two indices are proposed to evaluate power system robustness. The proposed indices are used to identify critical lines whose failure is due to overload, leading the power system to cascading outages and blackout. The first proposed index is a linear index. The second index is based on graph theory metrics. To prevent cascading outages, system robustness is calculated for all $N-1$ and $N-2$ contingencies. The lines whose outages lead to the smallest robustness values are considered as critical lines. The proposed indices are validated by applying to the IEEE 118-bus test system. Simulation results demonstrate the capability of both indices in identifying critical lines. Therefore, the purposed indices could be used as a reliable metric to apply preventive actions against possible cascading outages and blackouts.

Key words: Blackout, cascading failure, power system robustness, graph theory

1. Introduction

Despite great progress in the operation, control, and protection of power systems, the number of blackouts has increased dramatically. Due to the increasing demand for electricity and high penetration of renewable energy on one hand and the lack of sufficient expansion of transmission system owing to economic concerns on the other hand, much power system equipment and especially transmission lines are operated close to their maximum operation constraints [1]. Hence, a power system is exposed to serious overloads that decrease system robustness and security. Overloads cause cascading outages, which may lead a power system to large-scale blackout [1]. Detailed study of recent blackouts reveals that, generally, blackouts are triggered by an initial event, especially line outage. In other words, line tripping is a regular starting point of widespread blackouts. Subsequent events like misoperation of operators or protection system and load restoration can lead to further outages such as transmission line outages or generator outages [2]. Following the initial event in a heavily loaded system, power flow of the disconnected line is redistributed in the system and causes other lines to get overloaded. During overload conditions, the impedance trajectory may encroach on the 3^{rd} zone of distance relays and, therefore, some crucial transmission lines are undesirably disconnected. This process is repeated and leads to cascading outages and blackouts [3–7]. Therefore, power system robustness should be determined to identify contingencies that the system must be secured against [8].

Recently, there has been great effort to simulate cascading outages and blackouts. The OPA model considers two fast and slow iterative dynamic processes for cascading outage simulation [9–13]. OPA stands for Oak Ridge National Laboratory and Power Systems Engineering Research Center at the University of

[*]Correspondence: Farnaaz.hajbani@tabrizu.ac.ir

Wisconsin and University of Alaska to indicate the institutions collaborating to devise the simulation. In the case of overload, linear programming-based generation rescheduling and load shedding is applied. The branching process method proposes a probabilistic distribution function to determine the size of the blackout. This model gives the number of disconnected lines, as well as the amount of dropped load in each generation. However, it does not introduce any information about the mechanism of outages such as how, why, and which line is disconnected [14–19]. TRELSS, a computer program for transmission reliability evaluation of large-scale systems, evaluates the probabilistic reliability of the system. This computer program captures a cascading path starting from an aggravated system condition and initiating event [20, 21]. The stochastic model simulates all events randomly. In the case of overload alleviation, linear programing is used for generation rescheduling [22]. The newly proposed interaction model tries to evaluate components' failures impacts on each other. This model is too complicated and also time-consuming since it needs results of the OPA model [23]. Recently there has been great effort to study cascading outages of power systems as a complex network, based on structural properties [24–28]. In this method, the system is modeled as a graph with edges and nodes. The main objective of this model is to evaluate system robustness against cascading outages and blackouts, considering structural properties. The effect of load redistribution on system robustness was evaluated in [29, 30]. In this method, system load is assumed to be dependent on the node degree and number of nodes connected to the special node, while in the power system loads are independent of structure and are specified by users. The effect of node capacity on system robustness was studied in [31–36]. These works present the cascading outage of nodes as the main cause of blackouts and node capacity enlargement as a preventive action. However, bus triggering is a rare event in power systems and has been studied scarcely. In the meantime, transmission expansion is only possible by constructing new transmission lines, which is not applicable in short-term studies. The effect of loading level on system robustness was presented in [37]. In order to prevent cascading outages, loads of nodes encountering overload are transmitted to neighboring nodes, while in a power system, lines play this role. On top of that, transmitting the loads between bus bars is impossible in a power system. The criteria proposed for robustness calculation are not only structure-based, but also independent of power flow equations. Despite the mentioned differences, one remarkable feature of this model is its ability to calculate system robustness. This ability helps find nodes whose outages trigger cascading outages and blackouts.

The main objective of this paper is to present two indices for evaluating system robustness. The system robustness for normal, $N-1$, and $N-2$ contingencies is calculated using the indices. The lines whose outages decrease system robustness below the threshold value are considered as critical lines. The time domain analysis is performed in DigSILENT PowerFactory software and verifies the ability of the proposed indices in identifying the critical lines. Therefore, the purposed indices could be used as a reliable metric to apply preventive actions against possible cascading outages and blackouts. The proposed indices are applied to the IEEE 118-bus test system to demonstrate the performance of indices in large-scale systems. This test system has been used in many well-known publications in the field of power system operation and planning [38–41]. The remainder of this paper is organized as follows. Section 2 presents the proposed indices for robustness evaluation. Simulation results are presented in Section 3. In Section 4, a discussion on the proposed indices is presented. Finally, the conclusion is drawn in Section 5.

2. Evaluation of robustness

The scope of this paper is focused on identifying crucial transmission lines whose failure exposes the remaining lines to overload. Identification of these lines is performed by calculating power system robustness in all $N-1$

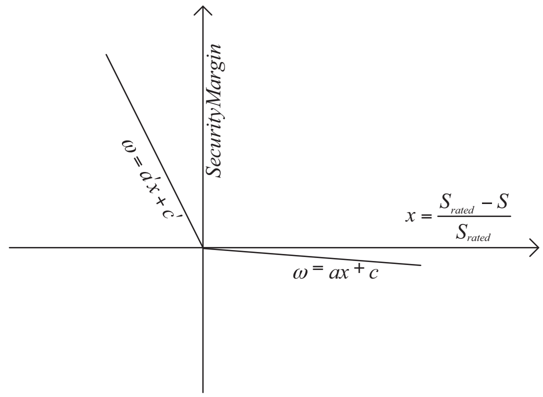

Figure 1. The schematic of designated weight.

and $N-2$ contingencies. Two indices are proposed for robustness calculation. The first index is a linear index. The second index is based on graph theory metrics. The proposed indices are evaluated as follows.

2.1. Robustness evaluation by linear index

The first index is calculated by a simple linear equation. The linear equation assigns a special weight to each line based on its loading level. Once the weights are calculated for each transmission line, the linear index is evaluated by summing all weights. Transmitted power on transmission lines changes due to topological changes such as line failure or generating unit outages. Regularly, power flow of the disconnected line is transmitted to its adjacent lines and increases their loading. In large-scale systems, while power flow increases in some transmission lines, it may decrease in some others. This issue results in misestimation of methods that use cumulative loading as a measure for overload estimation. Therefore, the proposed index should be able to recognize even fractional overload and should not be affected by power flow redistribution. Hence, the proposed linear index should introduce the following features:

1. The index should be able to recognize overload state in an L-line system when $L-1$ lines are loaded at minimum, while the remaining one is at excessive level.

2. The index should be able to identify the normal state of the system while all lines are heavily loaded but there is no overloaded one.

These two features illustrate the importance of allocated weight to the lines. The designated weight is derived by Eq. (1), as depicted in Figure 1. According to the figure, if the normalized difference between rated and actual apparent powers is smaller than the predefined security margin, the left axis line is used for weight designation. Otherwise, the right axis line is used.

$$\omega(l)=\begin{cases} a\frac{S_{rated}(l)-S(l)}{S_{rated}(l)}+c & if \quad \frac{S_{rated}(l)-S(l)}{S_{rated}(l)}>b \\ a'\frac{S_{rated}(l)-S(l)}{S_{rated}(l)}+c' & if \quad \frac{S_{rated}(l)-S(l)}{S_{rated}(l)}<b \end{cases} \tag{1}$$

Here, $\omega(l)$ is the assigned weight to line l; a, a' and c, c' are slopes and intercepts of the linear equations, respectively. b is the predefined security margin. $S_{rated}(l)$ and $S(l)$ stand for the rated and actual apparent powers of line l, respectively.

Once the weights are calculated, the linear index is evaluated by summing the weights according to Eq. (2).

$$LinearIndex = \sum_{l=1}^{L} \omega(l) \tag{2}$$

Here, l is the line number and L is the total number of lines in the system.

In this trend, if there is an overloaded line in the system, the linear index would be a large positive value; otherwise, it would be a small negative value. The unknown parameters a, a', c, and c' are selected such that they meet the mentioned features. Features 1 and 2 are mathematically expressed by Eqs. (3) and (4), respectively.

$$LinearIndex|_{1^{st} feature} = 1 \times a'(b - \varepsilon) + c' + (L-1) \times (a\frac{S_{rated} - S_{min}}{S_{rated}} + c) > 0 \tag{3}$$

$$LinearIndex|_{2^{nd} feature} = L \times (ab + c) < 0 \tag{4}$$

Here, $1 \times a'(b - \varepsilon) + c'$ expresses the fractional overload of only one transmission line and the term $(L-1) \times (a\frac{S_{rated} - S_{min}}{S_{rated}} + c)$ indicates that $L-1$ lines are loaded at the minimum loading level.

Loading of the least loaded line is defined as the minimum loading level. Since there is one overloaded line in the system, the index should be a positive value. S_{min} deals with the minimum loading level of line. ε is the fractional overload of the line expressed by Eq. (5). Eq. (4) indicates that all lines are loaded at the maximum level and there is no overloaded line. Therefore, the index should be a negative value.

$$\varepsilon = kb \tag{5}$$

Here, k is a small value within the $(0, 1)$ range.

Since even a fractional overload should be identified, a' should be much greater than a. Therefore, the relationship between a and a' is defined as below.

$$a' = Ka \tag{6}$$

Here, K is a large positive value. By substituting Eqs. (5) and (6) in Eq. (3), it is rewritten as Eq. (7).

$$Kab(1-k) + (L-1)(a\frac{S_{rated} - S_{min}}{S_{rated}}) + c' + (L-1)c > 0 \tag{7}$$

Here, K, k, a, and b are user-defined parameters.

Once user-defined parameters a and b are applied to Eq. (3), a proper range for c is obtained. Using the chosen value for c and applying it to Eq. (7), an interval to select an appropriate value for c' is achieved. In this manner, the unknown parameters of Eq. (3) are calculated in accordance with the requirements of the mentioned features. As the system loading increases, the linear index increases, as well. Hence, the system's capability to prevent cascading failures decreases. This issue illustrates the inverse relationship between the linear index and system robustness.

2.2. Robustness evaluation by graph theory metric

In graph theory, systems are represented as a network by $G(N, L)$, where N represents the number of nodes (buses in power system) and L represents the number of branches (transmission lines and transformers in the power system). In a graph, interconnection of nodes is represented by an adjacency matrix, which is a symmetric $N \times N$ matrix. The adjacency matrix just represents the existence of connection between nodes and gives no information on the number of links between nodes or strength of links. The weighted adjacency matrix, W, assigns a special weight to each of the nonzero elements of the adjacency matrix. The allocated weight to each link, w_{ij}, could be distance, cost, delay, or strength.

In order to study the graph robustness against cascading outage, a Laplacian matrix, Q, is utilized [42]. The elements of the Laplacian matrix are computed using the weighted adjacency matrix and diagonal matrix, Δ. The elements of the diagonal matrix are nonzero and computed by summing up the associated elements of each row of the weighted adjacency matrix as follows.

$$\delta_{ii} = \sum_{i=1}^{N} w_{ij} \tag{8}$$

Here, δ_{ii} are the diagonal elements of the diagonal matrix.

The Laplacian matrix is computed by means of the weighted adjacency matrix and diagonal matrix as below.

$$Q = \Delta - W \tag{9}$$

Eventually, elements of Laplacian matrix are figured by Eq. (10).

$$Q_{ij} = \begin{cases} \delta_{ij} & i = j \\ -w_{ij} & i \neq j \\ 0 & else \end{cases} \tag{10}$$

The eigenvalues of the Laplacian matrix give important information on system robustness against cascading outages. Since the sum of all elements in each row is zero, all of its eigenvalues are positive except the smallest one, which is zero. Effective graph resistance (EGR), one of the graph theory metrics for calculating system topological robustness, is derived by eigenvalues of the Laplacian matrix according to Eq. (12). The eigenvalues of the Laplacian matrix and EGR are represented by Eqs. (11) and (12), respectively.

$$\mu_1 \geq \mu_2 \geq ... \geq \mu_{N-1} \geq \mu_N \tag{11}$$

$$R_G = N \sum_{i=1}^{N-1} \frac{1}{\mu_i} \tag{12}$$

Here, R_G and μ_i are EGR and the eigenvalue of the Laplacian matrix, respectively.

The EGR gives important information about the system's topological robustness against cascading outages. A small value of EGR represents the immunity of the system against cascading outage, while a large value denotes its vulnerability.

If the system response to an initial event leads to overload of other transmission lines, the overloaded lines are exposed to failure. As the number of disconnected lines is increased, integrity of the power system is jeopardized and the system faces cascading outages and blackouts. Since the power system obeys Kirchhoff laws, the robustness calculation needs to consider fundamental rules of the power system. However, EGR just considers topological features of the system and its application in robustness evaluation needs to apply electrical rules to the topological features. To achieve this goal, a weight proportional to the apparent power of the lines is assigned to them. As the lines' loading exceeds the rated power, it becomes weak and vulnerable. To illustrate its weakness, the allocated weight should decrease as its apparent power exceeds its rated power. In this work, the elements of the weighted adjacency matrix are defined as in Eq. (13).

$$w_{ij} = \begin{cases} \frac{1}{a\frac{S_{rated}(l)-S(l)}{S_{rated}(l)}+c+Z} & if \ \frac{S_{rated}(l)-S(l)}{S_{rated}(l)} > b \\ \frac{1}{a'\frac{S_{rated}(l)-S(l)}{S_{rated}(l)}+c'+Z} & otherwise \end{cases} \tag{13}$$

Here, w_{ij} indicates the weight of line l, located between buses i and j.

According to Eq. (13), the allocated weight is the inverse of the designated weight by the linear index. The only difference is associated with the existence of Z. As mentioned earlier, the elements of W should be positive values. However, the linear index assigns a large positive value to the lines whose normalized differences are smaller than the predefined security margin; otherwise, it gives a small negative value. In order to satisfy the requirement of W, the linear equation should be shifted above the x-axis. This goal is achieved by introducing Z into Eq. (13). Once the parameters of the linear index are calculated, the value of the linear equation for $S(l) = S_{min}$ is evaluated. Since the difference between rated apparent power and actual power is greater than the predefined security margin, the linear equation would be negative. To shift the linear equation above the x-axis, the absolute of the evaluated value is selected as Z. Once the weighted adjacency matrix is calculated, diagonal and Laplacian matrices are derived using Eqs. (8) and (9), respectively.

In this trend, if the line is overloaded, its weight would be a small positive value close to zero, which indicates its vulnerability. Otherwise, it would be a positive value close to 1 that indicates its immunity against overload. In this manner, the EGR could be used as an index to study system robustness since electrical rules are applied to the topological features.

3. Simulation results

In order to apply the proposed robustness indices, the IEEE 118-bus test system is used as depicted in Figure 2. The IEEE 118-bus test system represents a simple approximation of the American electric power system (in the Midwest USA) as of December 1962. The IEEE 118-bus system contains 19 generators, 35 synchronous condensers, 176 lines, 10 transformers, and 91 loads. The AC power flow simulations and robustness calculations are accomplished in the DigSILENT/PowerFactory and MATLAB environments, respectively.

3.1. Robustness evaluation in $N-1$ and $N-2$ contingencies

In order to identify critical lines whose outages initiate cascading failure and blackout, system robustness is calculated for all $N-1$ and $N-2$ contingencies. The failures with the smallest robustness values are considered as the critical contingencies. The flowchart of critical line identification for $N-1$ contingencies, using the proposed EGR and linear index, is depicted in Figures 3a and 3b, respectively. As shown in Figures 3a and 3b, steps 1 through 4 are the same in both methods. Initially, both flowcharts calculate the system's initial state. Following an $N-1$ contingency, Y_{bus} of the system is updated and the apparent powers of the

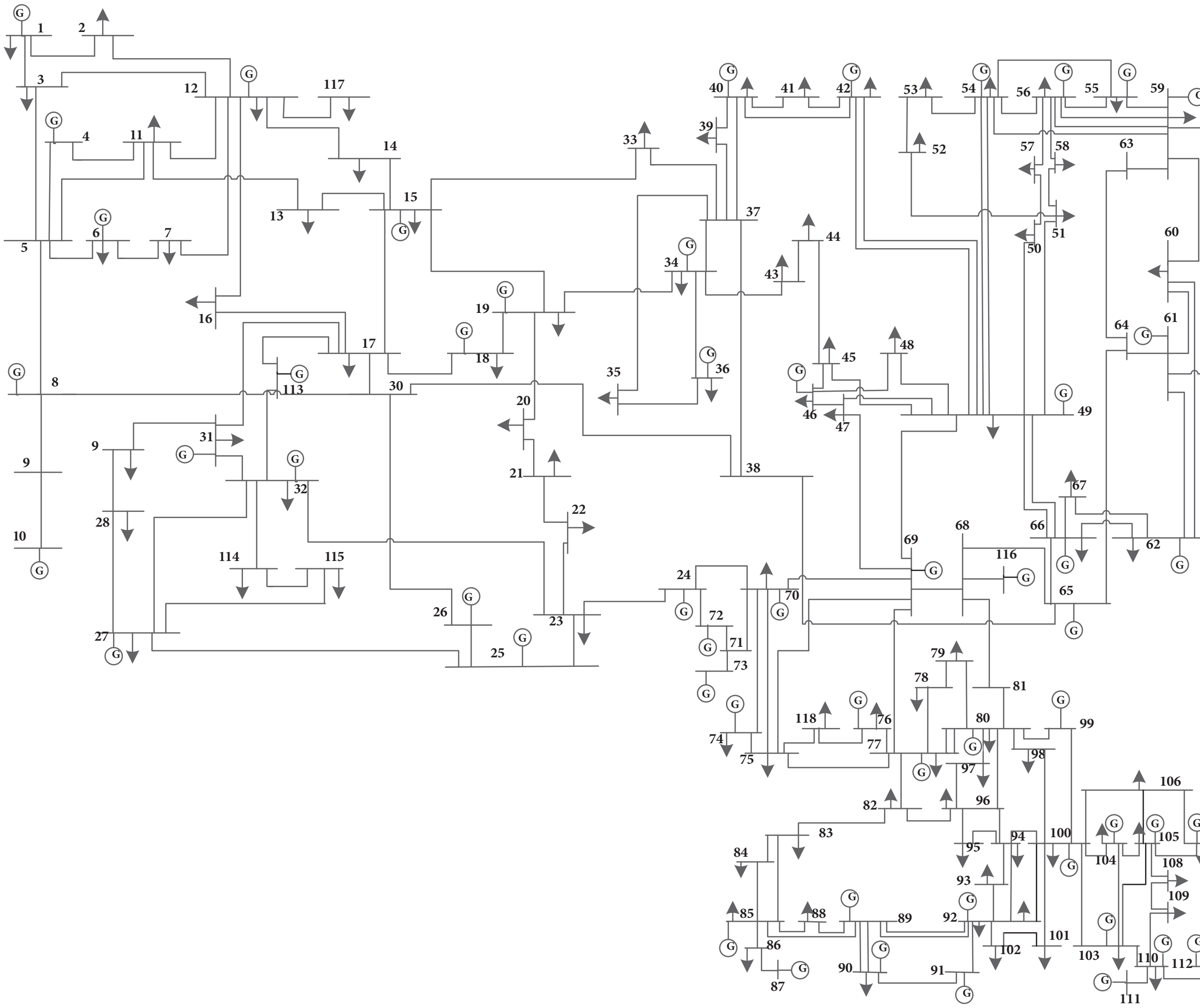

Figure 2. Diagram of IEEE 118-bus test system.

lines are evaluated. The linear index is evaluated by Eq. (2) for outage of line i. As previously mentioned in Section 2.1, the overloaded lines are given a positive weight but others are given a negative one. The zero that discriminates overloaded and nonoverloaded lines acts as a threshold for the linear index. Failures with positive index able to cause cascading failures are saved in the critical list but others with negative values are categorized as safe contingencies. Critical lines' identification by EGR requires the definition of a threshold. The threshold value is evaluated by computing the EGR index while all lines are loaded at their maximum level, i.e. 99.99%, and there is no overloaded line. The EGR threshold calculation steps are shown in Figure 3a. As depicted in Figure 3a, after evaluating the EGR for outage of line i, it is compared with the threshold of the EGR. If the EGR is greater than the threshold value, the outage is considered as a critical outage; otherwise, it is categorized in the safe list. In order to identify the critical lines using the linear index, a similar procedure is applied considering zero as the threshold, which is shown in Figure 3b. Therefore, once $N-1$ contingencies are simulated and related indices are evaluated, the contingencies are sorted based on the indices' values. Finally, the process ends with identification of critical lines.

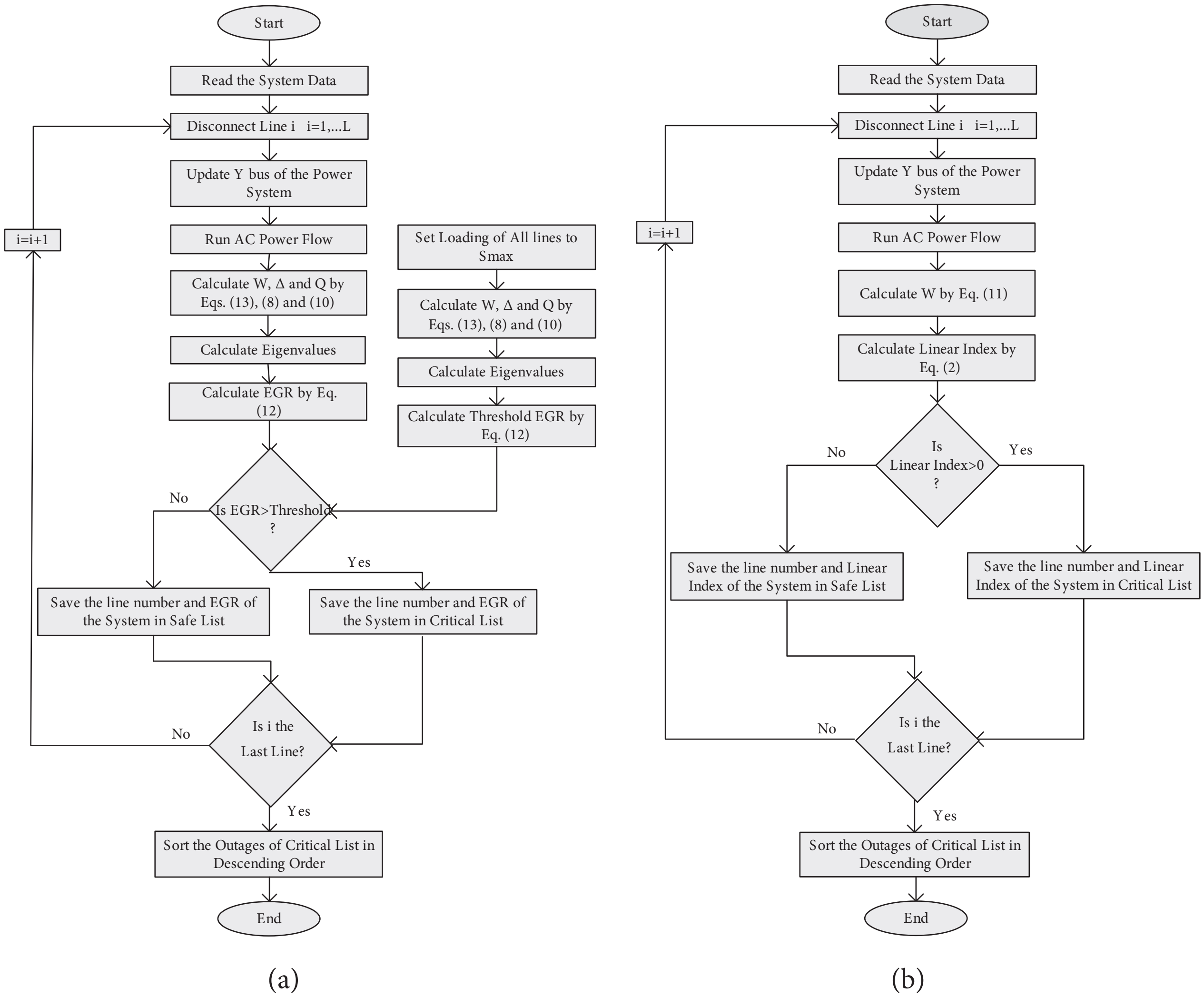

Figure 3. The flowchart of the critical line identification for $N-1$ contingencies: (a) critical line identification by EGR index; (b) critical line identification by linear index.

Simulation results for the normal state and all $N-1$ contingencies, based on linear and EGR indices, are depicted in Figures 4 and 5, respectively. Due to space limitation, just the worst 20 failures are shown. According to the results, the threshold value for linear and EGR indices are equal to zero and 11.0884, respectively. The linear and EGR indices for the system's normal state are equal to -16.967 and 2.122, respectively. The large gap between the threshold and normal state values declares the nonexistence of a heavily loaded line in the normal state, which is in accordance with the simulation results in DigSILENT PowerFactory.

According to Figure 4 and Figure 5, among all $N-1$ contingencies, just failure of line 26-30, shown by black bar, exposes the system to overload. The linear and EGR indices for other failures, shown by gray bars, are the same as normal state values. In other words, these contingencies cause no danger to the system's security. Both linear and EGR indices give the same result in identifying the critical line. However, the linear and EGR indices specify different rankings for the rest of the failures. Since these failures do not threaten system security, the difference is negligible.

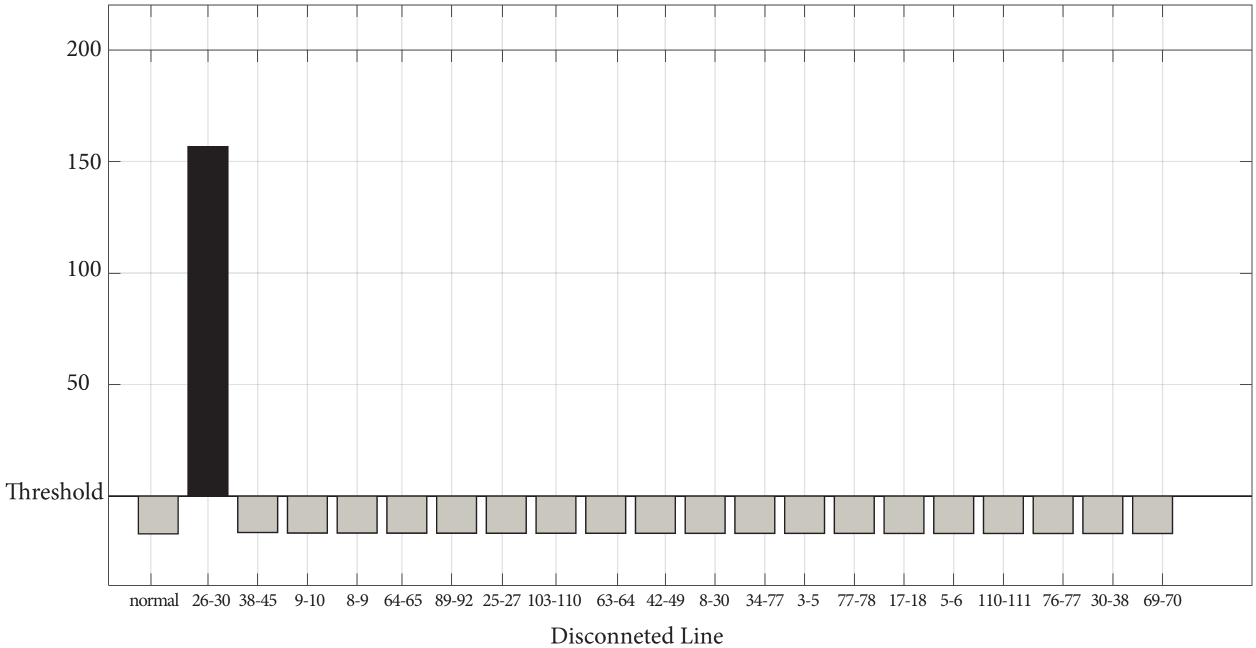

Figure 4. Linear index for $N-1$ contingencies.

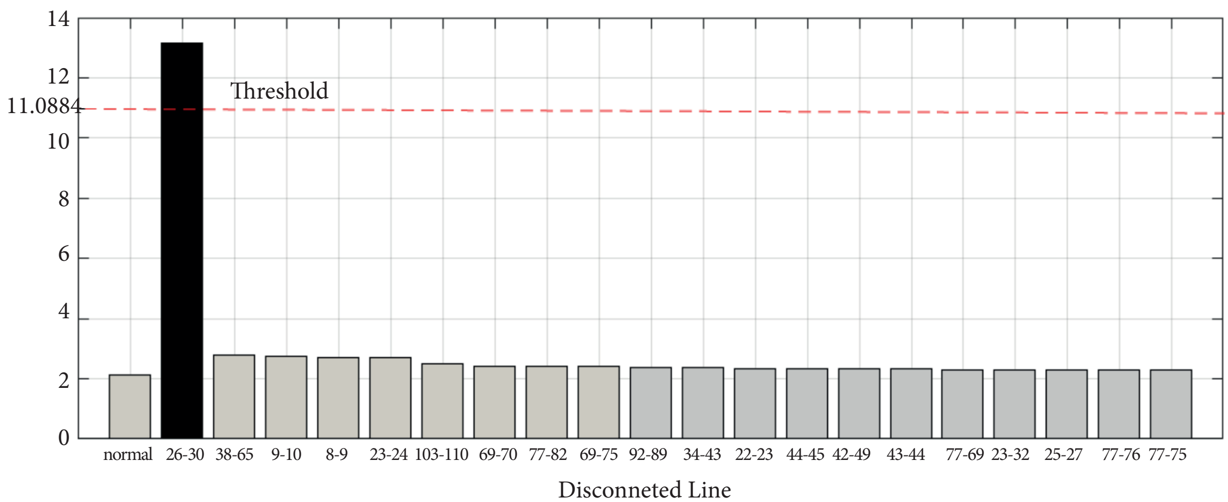

Figure 5. EGR index for $N-1$ contingencies.

For a system with 176 lines, there are $\binom{176}{2} = 15400$ second order outages. Among these outages, a small number of failures lead to overload. Simulation results of all overloaded $N-2$ contingencies based on linear and EGR indices are shown in Figure 6 and Figure 7, respectively. According to the figures, both metrics give the same result in identifying the worst five $N-2$ contingencies. Summary of $N-2$ contingencies is presented in Tables 1 and 2. The first and second dangerous failures are cascading outages of lines (26-30, then 25-27) and (26-30, then 23-25), respectively.

In $N-1$ contingencies, outage of line 26-30 is identified as the only failure that leads to overload of the system. According to Tables 1 and 2, the linear and EGR indices for the single outage of line 26-30 are equal

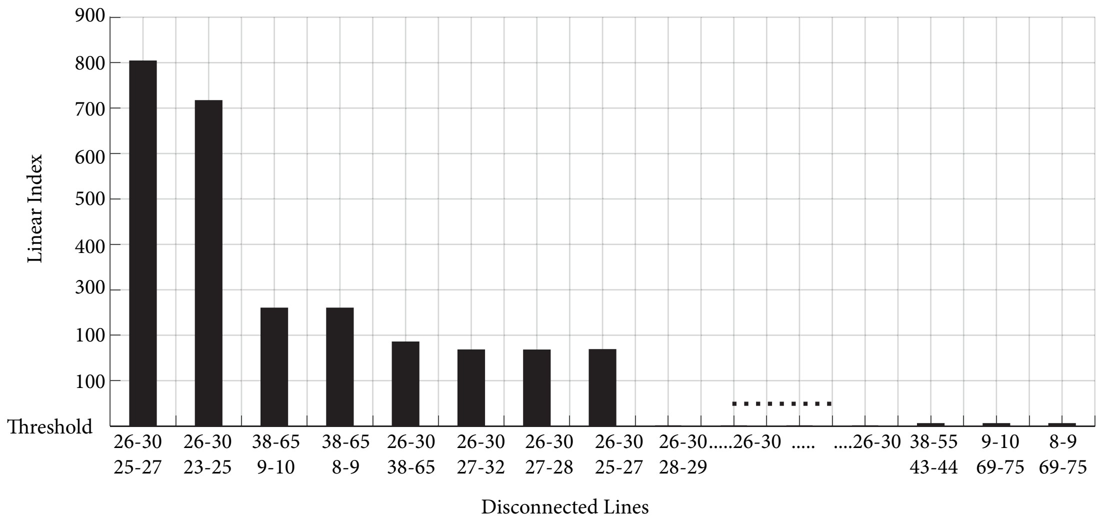

Figure 6. Linear index for all $N-2$ contingencies.

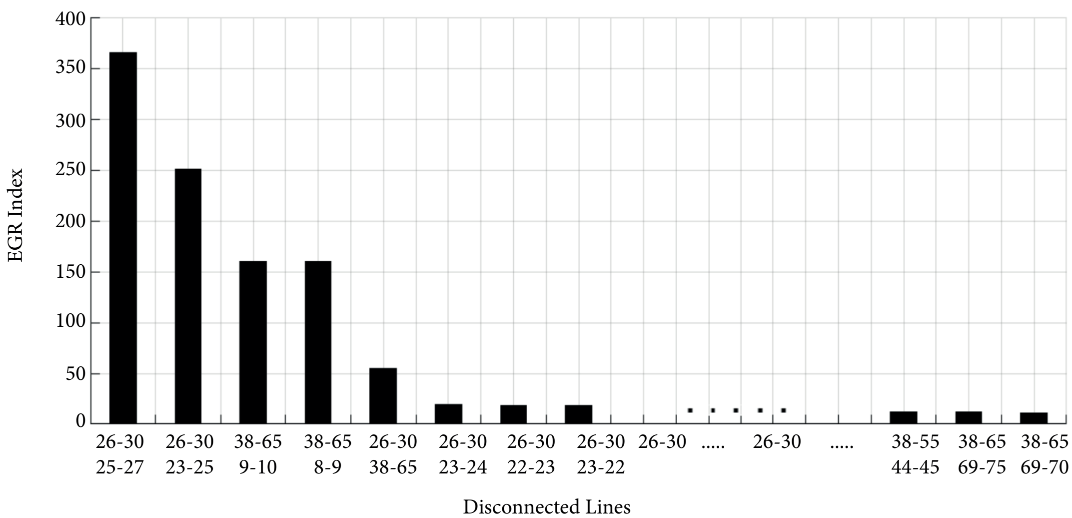

Figure 7. EGR index for all $N-2$ contingencies.

to 156.61 and 13.35, respectively. The linear and EGR indices for single outage of lines 25-27 and 23-25 do not exceed the threshold value. However, following cascading outages of lines (26-30, then 25-27) and (26-30, then 23-25), the EGR index increases to 365 and 251 and the linear index increases to 803.30 and 716.09, respectively. The deep gap between the indices for $N-1$ and $N-2$ contingencies demonstrates the perilous effect of cascading outages. The outages of lines (38-65, then 9-10) and (38-65, then 8-9) are ranked second and third, respectively. Following the single outage of the mentioned lines the system is not faced with overload since the linear and EGR indices do not exceed the threshold limit, according to Tables 1 and 2. Except for the first five failures, others are ranked differently. For the remaining outages, system security is close to line 26-30 outage. As previously mentioned, except line 26-30 failure, other single contingencies do not affect system security. Therefore, in these contingencies, outage of line 26-30 is the only cause of overload. Considering this issue and the fact that all demonstrated robustness values indicate overload existence in the system, the ranking difference is negligible. The failures at the end of the list include two groups: the first group includes one of

Table 1. Critical line identification regarding system robustness using EGR index.

Disconnected lines A, B	EGR index for cascading outage of lines A and B	EGR index for outage of line A	EGR index for outage of line B	Critical line/lines in cascading outage
26-30, 25-27	365	13.35>threshold	Lower than threshold	26-30, and 25-27
26-30, 23-25	365	13.35>threshold	Lower than threshold	26-30, and 23-25
38-65, 9-10	159.6	Lower than threshold	Lower than threshold	38-65, and 9-10
38-65, 8-9	159.6	Lower than threshold	Lower than threshold	38-65, and 8-9
⋮	⋮	⋮	⋮	⋮
26-30, 59-56	13.36	13.35>threshold	Lower than threshold	26-30
26-30, 15-33	13.36	13.35>threshold	Lower than threshold	26-30
⋮	⋮	⋮	⋮	⋮
38-65, 44-45	12.49	Lower than threshold	Lower than threshold	38-65, and 44-45
38-65, 69-75	12.33	Lower than threshold	Lower than threshold	38-65, and 69-75
38-65, 69-70	12.12	Lower than threshold	Lower than threshold	38-65, and 69-70

Table 2. Critical line identification regarding system robustness using linear index.

Disconnected lines A, B	Linear index for cascading outage of lines A and B	Linear index for outage of line A	Linear index for outage of line B	Critical line/lines in cascading outage
26-30, 25-27	803.3	156.61>threshold	Lower than threshold	26-30, and 25-27
26-30, 23-25	716.09	156.61>threshold	Lower than threshold	26-30, and 23-25
38-65, 9-10	259.27	Lower than threshold	Lower than threshold	38-65, and 9-10
38-65, 8-9	259.27	Lower than threshold	Lower than threshold	38-65, and 8-9
⋮	⋮	⋮	⋮	⋮
26-30, 49-50	156.68	156.61>threshold	Lower than threshold	26-30
26-30, 49-54	13.36	156.61>threshold	Lower than threshold	26-30
⋮	⋮	⋮	⋮	⋮
38-65, 43-44	5.44	Lower than threshold	Lower than threshold	38-65, and 43-44
9-10, 69-75	5.03	Lower than threshold	Lower than threshold	9-10, and 69-75
8-9, 69-75	5.03	Lower than threshold	Lower than threshold	8-9, and 69-75

lines 38-65, 8-9, or 9-10 outage. As depicted in Figures 4 and 5, since the single outage of lines 38-65, 8-9, or 9-10 increases the system loading level, they are considered as the basic reason for overload in the first group. The second group includes lines whose single outage does not increase system loading or does not threaten system security. However, cascading outage of these lines results in overload. This issue shows the importance of system analysis to identify lines whose cascading outages endanger system security.

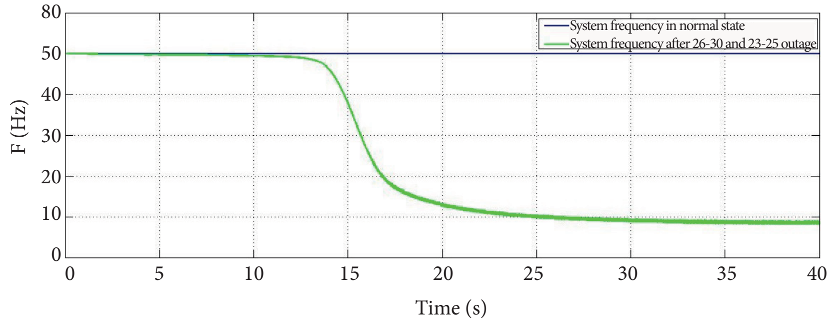

Figure 8. The frequency of the system in normal state and cascading outage of lines 26-30 and 23-25.

3.2. Time domain analysis

In order to verify the ability of the proposed indices in identifying critical contingencies, the sequence of cascading failures following the worst $N-2$ contingencies is simulated in DigSILENT PowerFactory. The system frequency for the normal state and the worst $N-2$ contingency is presented in Figure 8. Once lines 26-30 and 23-25 are disconnected at $t = 0.5s$, the loading of line 25-27 increases to 242.5%. The impedance trajectory of the relay encroaches into the third zone of the distance relay and leads to outage of the line at $t = 1.2s$. Once the line is tripped off, generating units 25 and 26 connected to the rest of the system through lines 26-30 and 25-27 and generating 5% and 7.17% of total generation of the system, respectively, are disconnected. Following these outages the system is divided into 6 electrical islands. Since there is not sufficient generation within the islands to meet electricity demand, further generating units are tripped off, leading the islands to blackout. The drop of the frequency indicates vulnerability of the system to the sequence of mentioned contingencies.

3.3. Critical line identification

Among the critical contingencies, there are a few lines that play a critical role in cascading failures and blackouts. Percentage of participation is defined as the ratio of failure numbers that each line participates in to the total failures that lead to cascading failures. The percentage of participation for lines participating in cascading failures is shown in Figure 9. The lines with percentage of participation lower than 0.5% are not shown. Accordingly, among all lines, line 26-30 has the greatest percentage of participation and events including line 26-30 lead to the lowest robustness value. Lines 38-65, 8-9, 9-10, and 42-49 are placed in the next stages. The failures that include line 42-49 outage are located at the end of the failure list and system robustness dose not decrease as much as for lines 8-9, 9-10, and 38-65. The lines 26-30, 38-65, 8-9, and 9-10 are considered as critical lines as their failure increases the system loading level and lead the system to cascading outage and blackout since they have the greatest percentage of participation and system robustness dramatically decreases following single and cascading outages of these lines. The obtained results from DigSILENT PowerFactory reveal the accuracy of the proposed indices in identifying critical lines whose failures due to overload lead the power system to cascading outages and blackout. Apart from identifying the critical lines, the ability to distinguish among different contingencies is another advantage of the proposed indices.

4. Discussion

This paper presents two indices for power system robustness evaluation in order to identify critical lines whose outages lead the system to cascading outages and blackout. The most significant advantages of this work are summarized as follows:

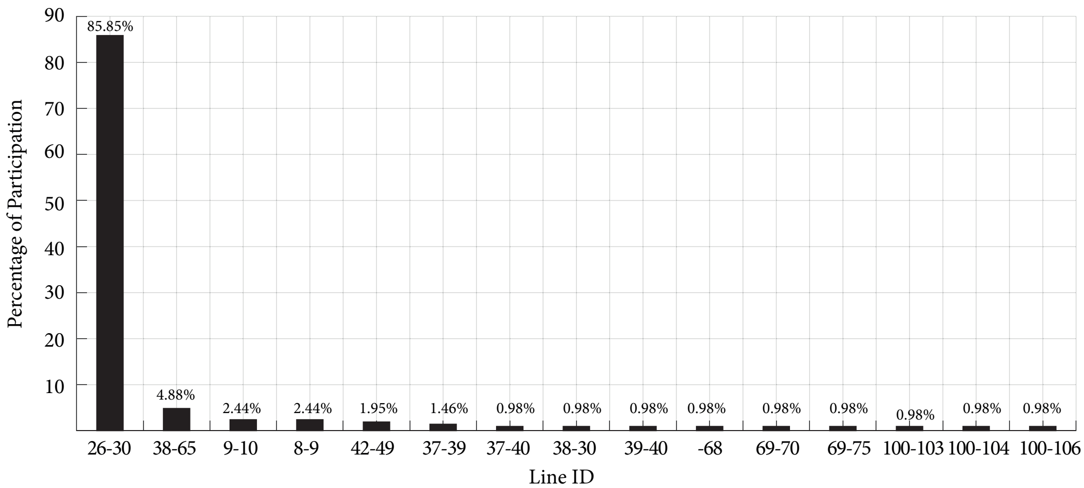

Figure 9. Percentage of participation of lines participating in failures leading to overload.

- The results of both indices in identifying the events that lead to cascading outage and blackout are in accordance with each other, according to more than 15,400 simulation results. In other words, although the linear index is much simpler than the mathematically based EGR index, it is capable of detecting the critical failures almost as accurately as the EGR index. Hence, the simple linear index is identified as an accurate and computationally efficient tool to recognize critical lines.
- The conventional methods presented for simulation of cascading outages are based on stochastic approaches that use complicated approaches for identifying the critical lines. However, the simplicity of the proposed indices is one of their advantages.
- The linear index is able to recognize even fractional overload in normal and overload states without being affected by power flow redistribution.
- By applying electrical rules to topological features, the EGR index, a well-known mathematically based index for evaluating system robustness based on topological features, is able to evaluate power system robustness.
- Both indices give the same result in ranking the most critical events. However, the remaining events have different rankings. The difference is ignorable since they have almost the same robustness value that indicates occurrence of overload in the system.
- The time domain analysis shows the accuracy of the indices in identifying critical lines.
- The percentage of participation reveals that some specific lines have the greatest impact on system robustness.
- Based on the accuracy and capability of the proposed indices in detection of critical lines, the indices could be applied to adopt preventive actions against possible cascading outages and blackouts.

5. Conclusion

In this paper two indices have been proposed for power system robustness evaluation in order to identify critical lines whose failures lead the power system to cascading outage and blackout. The first one is a linear index.

Parameters of this index are estimated based on two features. The first feature enables the index to identify even fractional overload. The second feature helps to distinguish between heavily loaded and overloaded states. The second index is based on graph theory, in which a special weight proportional to the line loading is assigned to the appropriate element of the related matrix. In this manner, the electrical information is applied to the topological features. The proposed indices are applied to the 118-bus test system using appropriate threshold values. The results for $N-1$ contingencies indicate that only one contingency jeopardizes system robustness. However, numerous $N-2$ contingencies decrease system robustness beneath the threshold. Analysis of the results illustrates that there are specific elements in the system whose cascading outage may lead to blackout although their single outage does not play such a role. On top of that, there are some specific lines that play critical roles in cascading outages and blackouts. The percentage of participation concept supports this claim. The results of both indices in identifying the worst $N-1$ and $N-2$ contingencies are the same. The percentage of participation reveals that only a small number of lines play critical roles in cascading outages and blackouts. According to the simulation results, the proposed indices could be used as effective tools for robustness evaluation and critical line identification in the power system. The drop of the frequency following the identified critical lines' outage also supports the ability of the purposed indices. Considering the ability of the indices in identifying critical lines, the indices could be used by operators to take preventive actions against possible cascading outages and blackouts.

Nomenclature

R_G	Effective graph resistance (EGR)	a, a'	Slopes of linear equations
LI	Linear index	c, c'	Intercepts of linear equations
Q	Laplacian matrix	b	Predefined security margin
Δ	Diagonal matrix	S_{rated}	Rated power
W	Weighted adjacency matrix	S	Apparent powers
μ_i	Eigenvalue of Q	L	Total number of lines
l	Line number	K	Large positive value (user-defined)
k	User-defined value in $(0,1)$	δ_{ii}	Elements of Δ
Z	Absolute of linear equation for $S(l)=S_{min}$		

References

[1] Venkatasubramanian MV, Kezunovic M, Vittal V. Detection, Prevention and Mitigation of Cascading Events. Madison, WI, USA: Power Systems Engineering Research Center, 2008.

[2] UCTE. Final Report on the Disturbances of 4 November 2006. Brussels, Belgium: UCTE, 2007.

[3] Turkish Electricity Transmission Company. Turkish Power System and 31st March 2015 Blackout. SEERC Management Board Meeting. Ankara, Turkey: Turkish Electricity Transmission Company, 2015.

[4] Liscouski B, Elliot W. Final Report on the August 14, 2003 Blackout in the United States and Canada: Causes and Recommendations. A Report to US Department of Energy. Washington, DC, USA: Department of Energy, 2004.

[5] NERC Steering Group. Technical Analysis of the August 14, 2003, Blackout: What Happened, Why, and What Did We Learn. Report to the NERC Board of Trustees. Atlanta, GA, USA: NERC, 2004.

[6] Andersson G, Donalek P, Farmer R, Hatziargyriou N, Kamwa I, Kundur P. Causes of the 2003 major grid blackouts in North America and Europe, and recommended means to improve system dynamic performance. IEEE T Power Syst 2005; 20: 1922-1928.

[7] UCTE. Final Report of the Investigation Committee on the 28 September 2003 Blackout in Italy. Brussels, Belgium: UCTE, 2004.

[8] Xu C, Gu W, Luo L, Yao J, Yang Sh, Wang K, Zeng D, Fan M. An interval-based contingency selecting approach considering uncertainty. Turk J Elec Eng & Comp Sci 2016; 24: 4682-4692.

[9] Dobson I, Carreras BA, Lynch VE, Newman DE. An initial model for complex dynamics in electric power system blackouts. In: Hawaii International Conference on System Sciences; 2001.

[10] Carreras BA, Newman DE, Dobson I, Degala NS. Validating OPA with WECC data. In: Hawaii International Conference on System Sciences; 2013.

[11] Ren H, Dobson I, Carreras BA. Long-term effect of the n-1 criterion on cascading line outages in an evolving power transmission grid. IEEE T Power Syst 2008; 23: 1217-1225.

[12] Zeng K, Wen J, Cheng S, Lu E, Wang N. A Critical Lines Identification Algorithm of Complex Power System. In: Hawaii International Conference on System Sciences; 2001

[13] Karimi E, Ebrahimi A. Probabilistic transmission expansion planning considering risk of cascading transmission line failures. Int T Electr Energy 2015; 25: 2547-2561.

[14] Kim J, Wierzbicki KR, Dobson I, Hardiman RC. Estimating propagation and distribution of load shed in simulations of cascading blackouts. IEEE J Syst 2012; 6: 548-557.

[15] Ren H, Dobson I. Using transmission line outage data to estimate cascading failure propagation in an electric power system. IEEE T Circuits Syst 2008; 55: 927-931.

[16] Dobson I. Estimating the propagation and extent of cascading line outages from utility data with a branching process. IEEE T Power Syst 2012; 27: 2146-2155.

[17] Kim J, Dobson I. Approximating a loading-dependent cascading failure model with a branching process. IEEE T Reliab 2010; 59: 691-699.

[18] Qi J, Dobson I, Mei S. Towards estimating the statistics of simulated cascades of outages with branching processes. IEEE T Power Syst 2013; 28: 3410-3419.

[19] Ren H, Dobson I. Using transmission line outage data to estimate cascading failure propagation in an electric power system. IEEE T Circuits Syst 2008; 55: 927-931.

[20] Phadke AG, Thorp JS. Expose hidden failures to prevent cascading outages. IEEE Comput Appl Pow 1996; 9: 20-23.

[21] Kumbale M, Hardiman R, Makarov Y. A methodology for simulating power system vulnerability to cascading failures in the steady state. Eur T Elect Power 2008; 18: 802-808.

[22] Anghel M, Werley KA, Mottor AE. Stochastic model for power grid dynamics. In: Hawaii International Conference on System Sciences; 2007.

[23] Qi J, Sun K, Mei S. An interaction model for simulation and mitigation of cascading failures. IEEE T Power Syst 2015; 30: 804-819.

[24] Wang JW, Rong LL. A model for cascading failures in scale-free networks with a breakdown probability. Physica A 2009; 388: 1289-1298.

[25] Weia DQ, Luoa XS, Zhang B. Analysis of cascading failure in complex power networks under the load local preferential redistribution rule. Physica A 2012; 391: 2771-2777.

[26] Koç Y, Warniera M, Mieghemb PV, Kooij RE, Brazier MT. A topological investigation of phase transitions of cascading failures in power grids. Physica A 2014; 415: 273-284.

[27] Bompard E, Napoli R, Xue F. Extended topological approach for the assessment of structural vulnerability in transmission networks. IET Gener Transm Dis 2010; 4: 716-724.

[28] Arianos S, Bompard E, Carbone A, Xue F. Power grid vulnerability: a complex network approach. Chaos 2009; 19: 13119.

[29] Bao ZJ, Cao YJ, Wang GZ, Ding LJ. Analysis of cascading failure in electric grid based on power flow entropy. Phys Lett A 2009; 373: 3032-3040.

[30] Koç Y, Warniera M, Mieghemb PV, Kooij RE, Brazier MT. The impact of the topology on cascading failures in a power grid model. Physica A 2014; 402: 169-179.

[31] Li DD, Dong LX, Yue WX, Hua OYD, Bin Z. Critical thresholds for scale-free networks against cascading failures. Physica A 2014; 416: 252-258.

[32] Wang J. Robustness of complex networks with the local protection strategy against cascading failures. Safety Sci 2013; 53: 219-225.

[33] Wang J. Mitigation strategies on scale-free networks against cascading failures. Physica A 2013; 392: 2257-2264.

[34] Wang JW, Rong LL. Robustness of the western United States power grid under edge attack strategies due to cascading failures. Safety Sci 2011; 49: 807-812.

[35] Fang X, Yang Q, Yan W. Modeling and analysis of cascading failure in directed complex networks. Safety Sci 2014; 65: 1-9.

[36] Koc Y, Warnier M, Kooij RE, Brazier FM. An entropy based metric to quantify the robustness of power grids against cascading failures. Safety Sci 2013; 59: 126-134.

[37] Bompard E, Napoli R, Xue F. Analysis of structural vulnerabilities in power transmission grids. Int J Crit Infr Prot 2009; 2: 5-12.

[38] Xu X, Yan Z, Shahidehpour M, Wang H, Chen S. Power system voltage stability evaluation considering renewable energy with correlated variabilities. IEEE T Power Syst 2018; 33: 3236-3245.

[39] Chen H, Fang X, Zhang R, Jiang T, Li G, Li F. Available transfer capability evaluation in a deregulated electricity market considering correlated wind power. IET Gener Transm Dis 2018; 12: 53-61.

[40] Pena I, Anido C, Hodge B. An extended IEEE 118-bus test system with high renewable. IEEE T Power Syst 2018; 33: 281-289.

[41] Liu X, Wen Y, Li Z. Multiple solutions of transmission line switching in power systems. IEEE T Power Syst 2018; 33: 1118-1120.

[42] Mieghem PV. Graph Spectra for Complex Networks. Cambridge, UK: Cambridge University Press, 2011.